ARMY RESEARCH LABORATORY

Enhancement of Target Contrast in Polarimetric Imagery Using Image Fusion

by Melvin Felton and Kristan Gurton

ARL-TR-5176 **April 2010**

NOTICES

Disclaimers

The findings in this report are not to be construed as an official Department of the Army position unless so designated by other authorized documents.

Citation of manufacturer's or trade names does not constitute an official endorsement or approval of the use thereof.

Destroy this report when it is no longer needed. Do not return it to the originator.

Army Research Laboratory
Adelphi, MD 20783-1197

ARL-TR-5176 **April 2010**

Enhancement of Target Contrast in Polarimetric Imagery Using Image Fusion

Melvin Felton and Kristan Gurton
Computational and Information Sciences Directorate, ARL

REPORT DOCUMENTATION PAGE	Form Approved OMB No. 0704-0188

1. REPORT DATE *(DD-MM-YYYY)*	2. REPORT TYPE	3. DATES COVERED (From - To)
April 2010	Summary	

4. TITLE AND SUBTITLE
Enhancement of Target Contrast in Polarimetric Imagery Using Image Fusion

5a. CONTRACT NUMBER

5b. GRANT NUMBER

5c. PROGRAM ELEMENT NUMBER

6. AUTHOR(S)
Melvin Felton and Kristan Gurton

5d. PROJECT NUMBER

5e. TASK NUMBER

5f. WORK UNIT NUMBER

7. PERFORMING ORGANIZATION NAME(S) AND ADDRESS(ES)
U.S. Army Research Laboratory
ATTN: RDRL-CIE-S
2800 Powder Mill Road
Adelphi, MD 20783-1197

8. PERFORMING ORGANIZATION REPORT NUMBER
ARL-TR-5176

9. SPONSORING/MONITORING AGENCY NAME(S) AND ADDRESS(ES)

10. SPONSOR/MONITOR'S ACRONYM(S)

11. SPONSOR/MONITOR'S REPORT NUMBER(S)

12. DISTRIBUTION/AVAILABILITY STATEMENT
Approved for public release; distribution unlimited.

13. SUPPLEMENTARY NOTES

14. ABSTRACT
We have examined the use of two statistical/numerical image fusion techniques for polarimetric imagery that each allow for an objective analysis of the resultant data products. The first technique is principal component analysis (PCA), a standard multivariate image processing method used to redistribute the information within the data set and possibly reduce the dimensions of the data set. The second method fuses conventional thermal imagery with a novel data product, the enhanced degree-of-linear polarization (DOLP). We performed receiver operating characteristic (ROC) curve analysis to quantify the resultant contrast between the manmade objects in the scene and the natural backgrounds. We found that the PCA data products inconsistently conveyed the desired contrast information, and that ROC curve analysis is not well suited to quantify the contrast in the PCA imagery. On the other hand, fusing the conventional thermal and the enhanced DOLP images provided a robust data product that effectively combines the information provided by the sensor.

15. SUBJECT TERMS
Target contrast, image fusion, polarimetric imaging

16. SECURITY CLASSIFICATION OF:			17. LIMITATION OF ABSTRACT	18. NUMBER OF PAGES	19a. NAME OF RESPONSIBLE PERSON
a. REPORT	b. ABSTRACT	c. THIS PAGE	UU	26	Melvin Felton
Unclassified	Unclassified	Unclassified			19b. TELEPHONE NUMBER (*Include area code*) (301) 394-2618

Contents

List of Figures iv

List of Tables iv

Acknowledgments v

1. Introduction 1

2. Experiment 2

3. Image Fusion 3

3.1 Principal Component Analysis (PCA) 3

3.2 Enhanced DOLP and S_0 4

3.3 ROC Curve Analysis 5

4. Results 6

4.1 PCA 6

4.2 Fused S_0 and Enhanced DOLP 9

5. Conclusion 13

6. References 15

List of Symbols, Abbreviations, and Acronyms 16

Distribution List 17

List of Figures

Figure 1. Target site with two surrogate tanks and natural background. 3
Figure 2. Image of the test scene with the pixels considered to comprise the target outlined in red. The remainder of the image is designated as the background. 6
Figure 3. Diurnal ROC curve analysis for PC 1. 7
Figure 4. Diurnal ROC curve analysis for PC 2. 7
Figure 5. Diurnal ROC curve analysis for PC 3. 8
Figure 6. Environmental parameters measured during the test. 8
Figure 7. Diurnal DOLP and enhanced DOLP ROC curve analysis. 10
Figure 8. DOLP (a) and enhanced DOLP (b) images taken at 0:00. 11
Figure 9. DOLP (a) and enhanced DOLP (b) images taken at 13:00. 11
Figure 10. Diurnal S_0 and fused S_0-enhanced DOLP ROC curve analysis. 12
Figure 11. S_0 (a) and fused S_0-enhanced DOLP (b) images taken at 0:00. 12
Figure 12. DOLP (a), enhanced DOLP (b), S_0 (c), and fused S_0-enhanced DOLP (d) images taken at 23:50. 13

List of Tables

Table 1. Polarimetric sensor data products. 2

Acknowledgments

This work was accomplished using data from the Hyperspectral and Polarimetric Target Detection Program at the Precision Armament Laboratory (PAL) Tower at the Armament Research and Development Engineering Center (ARDEC) with the help of Mr. Joao Romano (Program Manager), Mr. Mark Woolley (PAL Manager), and Zed Habte (test engineer).

INTENTIONALLY LEFT BLANK

1. Introduction

Thermal imagers have been established as the primary tool in military and security activities that involve surveillance, targeting and tracking, and night-time operations. Unlike I^2 devices, which depend on ambient light levels, thermal imagers create pseudo-images of given scenes based on thermal emissions, exploiting the fact that all objects with a temperature above 0 K emit thermal radiation. Contrast between the objects within a thermal image is determined by their effective temperatures, which are a function of their true temperature and emissivity, a characteristic that describes how efficiently an object radiates energy compared to a blackbody. If a target and the background have the same effective temperature, there is no thermal contrast between them and it is impossible to distinguish the two in a thermal image. The diurnal cycles of the thermal properties of both manmade and natural objects tend to bring about periods of low contrast within thermal images, often referred to as thermal crossovers or inversion periods (*1*). These inversion periods tend to occur during periods of rapidly changing temperatures, such as sunrise and sunset, but may occur at any time throughout the day, depending on both temperature differences between objects and their backgrounds, and on environmental factors, such as solar loading, cloud cover, winds, etc.

Thermal polarimetric imaging has been proposed as a method to enhance conventional thermal imaging (*2*). It creates images of a scene that are based on the states of polarization of the infrared (IR) light emitted or reflected from the objects within the scene. An object's polarimetric signature is a function of its surface geometry and roughness. Due to the different geometrical and roughness features associated with objects constituting natural backgrounds and manmade objects, the polarization states of the thermal light forming an image can be used as a discriminator between objects of interest and background clutter. Using the polarization of the light, it is frequently possible to obtain an image of a scene that has polarimetric contrast between objects and their backgrounds, even when there is no thermal contrast.

The ability of thermal polarimetric imaging to enhance conventional thermal imaging produces a need for an efficient method to combine, or fuse, the two channels of information. Basic overlays of polarimetric data products onto conventional thermal imagery can help distinguish manmade objects from the natural background. In addition to improved discrimination between these objects and their backgrounds, colorimetric overlays provide more specific information—e.g., horizontal and vertical states of polarization, Stokes parameter values, degree-of-linear polarization (DOLP), etc (*3*, *4*). The process of assessing the quality of these overlay-based fused data products is very subjective because the data underlying the imagery is not fused—only the final images. In this sense, the term "fused" merely refers to the effect of the overlay on human perception of the resultant image. In this study, we examine two statistical/numerical image fusion techniques that each allow for an objective analysis of their resultant data

products. The first technique is principal component analysis (PCA), a standard multivariate image processing method used to redistribute the information within the data set and possibly reduce the dimensions of the data set. The second method fuses conventional thermal imagery to a novel data product, the enhanced DOLP. Receiver operating characteristic (ROC) curve analysis is performed to quantify the resultant improved contrast between the manmade objects in the scene and the natural backgrounds.

2. Experiment

The sensor used is a long-wave IR (LWIR) microbolometer-based rotating retarder imaging polarimeter developed by Polaris Sensor Technologies, Inc., Huntsville, AL (*5*). It operates by capturing images sequentially in time, each at a different orientation of a rotating retarder. Together, the retarder and linear polarizer act as a polarization state analyzer for the light forming the image. Using the data reduction matrix method, the Stokes vectors are calculated, which completely characterizes the polarization states of the light from the scene. Table 1 lists the definitions of the data products provided by the imager and processing hardware. This study only examined linear states of polarization, so the S_3 Stokes vector is omitted from table 1.

Table 1. Polarimetric sensor data products.

Measured image	Description
S_0	Radiance image, W/cm^2-sr
S_1	Horizontally polarized radiance minus vertically polarized radiance, W/cm^2-sr
S_1/ S_0	S_1 image normalized by radiance image, S_0
S_2	45° polarized radiance minus 135° polarized radiance, W/cm^2-sr
S_2/ S_0	S_2 image normalized by radiance image, S_0
DOLP	Degree of linear polarization, $\sqrt{S_1^2 + S_2^2}/S_0$

The test was conducted at the Precision Armaments Laboratory located in Picatinny Arsenal, NJ. The camera was situated on the sixth floor of a tower (approximately 200 ft high), looking out of the windows towards the target site, which was at approximately 0.5 km in range and contained two surrogate tanks and natural backgrounds including grass, brush, and trees (figure 1). In addition to the 200 ft elevation of the sixth floor of the tower, the tower, itself, was situated on top of a ridge approximately 175 ft above the target site.

Figure 1. Target site with two surrogate tanks and natural background.

Environmental measurements available at the target site include air temperature, relative humidity, ceilometer data, and pyrgeometer (precision infrared radiometer [PIR]) data. The ceilometer provides real-time reports of cloud bases and depths directly above the ceilometer, and determines cloud cover by using a weighted average of 30-s cloud hit reports over a 30-min period. The pyrgeometer measured ambient LWIR radiation from 3–50 μm within a 2π steradian field of view. A direct comparison of ceilometer and pyrgeometer data revealed that the baseline reading for a cloudless daytime sky was roughly 275–280 W/m^2. Any value higher than this typically indicates the presence of clouds such that the higher the value, the thicker the cloud cover. During this study, sunrise and sunset occurred at roughly 0500 and 2000, respectively.

The data acquisition clocks for the environmental data and the camera were synced to enable retrieval of coincident data. The temporal resolutions of the data are: air temperature, relative humidity, and pyrgeometer—2 s; ceilometer—10 s; and camera—10 min. Data was acquired continuously between 0000 and 2300 on May 13, 2009.

3. Image Fusion

3.1 Principal Component Analysis (PCA)

PCA may be used as a multivariate image analysis technique (*6*). Principal components (PCs) refer to derived variables that are a linear combination of the original variables. PCA redistributes the information of the original data set of correlated variables so that each resultant PC is uncorrelated. The weight applied to each of the original variables in the sum forming the linear combination is determined by the statistical properties of the original variables. The original variables are often standardized, i.e., each variable is mean subtracted and divided by

its standard deviation to place equal importance on the variables in the data set, especially when the variables vary significantly in magnitude or are measured in different units. The PCA process calculates the eigenvalues and eigenvectors of the covariance matrix of this standardized data set.

The eigenvectors are ordered according to the descending order of the magnitude of their corresponding eigenvalues. Because the eigenvalues correspond to the variance of the eigenvector components, organizing the eigenvectors in this fashion ensures that the first PC will contain the largest percentage of the variance of the data set, the second principal component will contain the second largest percentage of the variance, and so on.

PCA is a form of image fusion because each PC image is a linear combination of the original imagery channels. Furthermore, because these principal components are uncorrelated, each PC image should convey predominantly different information. Note that although we are interested in contrast improvement between target and background in this study, this may not be the only or even the most significant information within the data. Therefore, it is unknown which component will contain this contrast information during any given measurement.

3.2 Enhanced DOLP and S_0

The DOLP is the percentage of the image forming light that is linearly polarized. The numerator in the expression for DOLP (see table 1) is analogous to a Euclidean distance metric, having the components S_1 and S_2. It is common for the scene being imaged to consist of more horizontally and/or vertically oriented surfaces than ±45° surfaces. For these scenes, the DOLP will be dominated by the S_1 component and, therefore, the information in the DOLP image will closely mimic the information in the S_1 image. This does not mean that there is no useful information in the S_2 image. A data product analogous to DOLP that retains this information can be obtained by using standardized S_1/S_0 and standardized S_2/S_0. This places equal importance on the S_1 and S_2 information. We refer to this new data product as an enhanced DOLP image (see equation 1). In this expression, μ and σ refer to the mean and standard deviation, respectively, and $S_1^{'} = S_1/S_0$ and $S_2^{'} = S_2/S_0$ refer to the normalized S_1 and S_2 images, respectively.

$$enhanced\ DOLP = \sqrt{\left(\frac{S_1^{'} - \mu_{S_1^{'}}}{\sigma_{S_1^{'}}}\right)^2 + \left(\frac{S_2^{'} - \mu_{S_2^{'}}}{\sigma_{S_2^{'}}}\right)^2} \quad (1)$$

The term “enhanced” refers both to the ability of this data product to convey more information on average than the traditional DOLP, and to the improved signal-to-noise ratio that results from using standardized variables (*7*).

The fused enhanced DOLP and S_0 image is simply the sum of the standardized S_0 image and a scaled version of the enhanced DOLP image. The scaling of the enhanced DOLP image is such that each pixel is multiplied by the fraction of the image’s dynamic range that it represents.

Therefore, pixels with large values of enhanced DOLP will be weighted more heavily than those with lower values. The result is an image that now contains S_0 information, as well as information pertaining to the sources of linearly polarized light in the scene.

3.3 ROC Curve Analysis

ROC curve analysis provides a useful metric for assessing the ability to distinguish between a target and its background based on the separation of their histograms. For a 256-point histogram, 256 bins between the maximum and minimum values of an image are formed. Each bin corresponds to a threshold value at which the overlap between the target histogram and the background histogram is assessed. The area under the ROC curve is a measure of the separation of target and background histograms throughout the whole range of 256 thresholds. It represents the probability that a pixel will be correctly classified as target or background (*8*).

ROC curve analysis is useful for determining target detectability, but it has its limitations. It must be remembered that ROC curves assess how well a target can be distinguished from its background based solely on their respective pixel values. ROC curves do not take into account the tendency of objects in a scene to result in the clustering of image pixels with similar values. This clustering of pixels with similar values makes it possible for a target to be distinguished from its background, even if portions of the background contain similar values to the target. The results of ROC curve analysis in such a situation may inaccurately suggest that there is no contrast between target and background.

The target and the background have to be clearly defined for ROC curve analysis to be performed on an image. Figure 2 is an image of the test scene with the target outlined in red. In this study, all manmade objects in the scene are considered to comprise the target, i.e., two surrogate tanks, pavement, and mobile calibration source beneath a protective covering sitting on the paved pathway. Everything outside of these regions—e.g., trees, grass, and brush—is considered as the background. The total numbers of pixels comprising the target and background are 524 and 34,584, respectively.

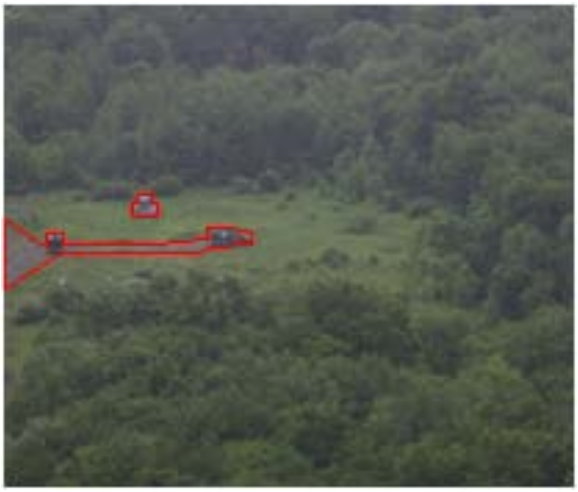

Figure 2. Image of the test scene with the pixels considered to comprise the target outlined in red. The remainder of the image is designated as the background.

4. Results

4.1 PCA

The PCA was performed on a three-variable (S_0, S_1, and S_2) data set. The diurnal plots of the area under the ROC curve for the three PC images are shown in figures 3, 4, and 5, and each show a large amount of variation that is correlated with each other. In particular, periods of high area under the curve for one PC image are accompanied by periods of low area under the curve in one or the other PC images. The shifts in these periods of high area under the curve to low area under the curve often occur abruptly. The frequency of these shifts does not appear to correlate with the environmental parameters measured during this study (figure 6). For example, between 0000 and 0600, temperatures were less than 5 °C and slowly decreasing, and the pyrgeometer indicated clear skies, yet the ROC curve analysis shows that high values of area under the ROC curve alternates randomly between the PC 1 and PC 2 images. The most notable relationships between PC image ROC curve analysis and the environmental factors are the direct correlation between PC 3 area under the curve and temperature profiles, and the slight inverse correlation between PC 1 area under the curve and ambient IR loading.

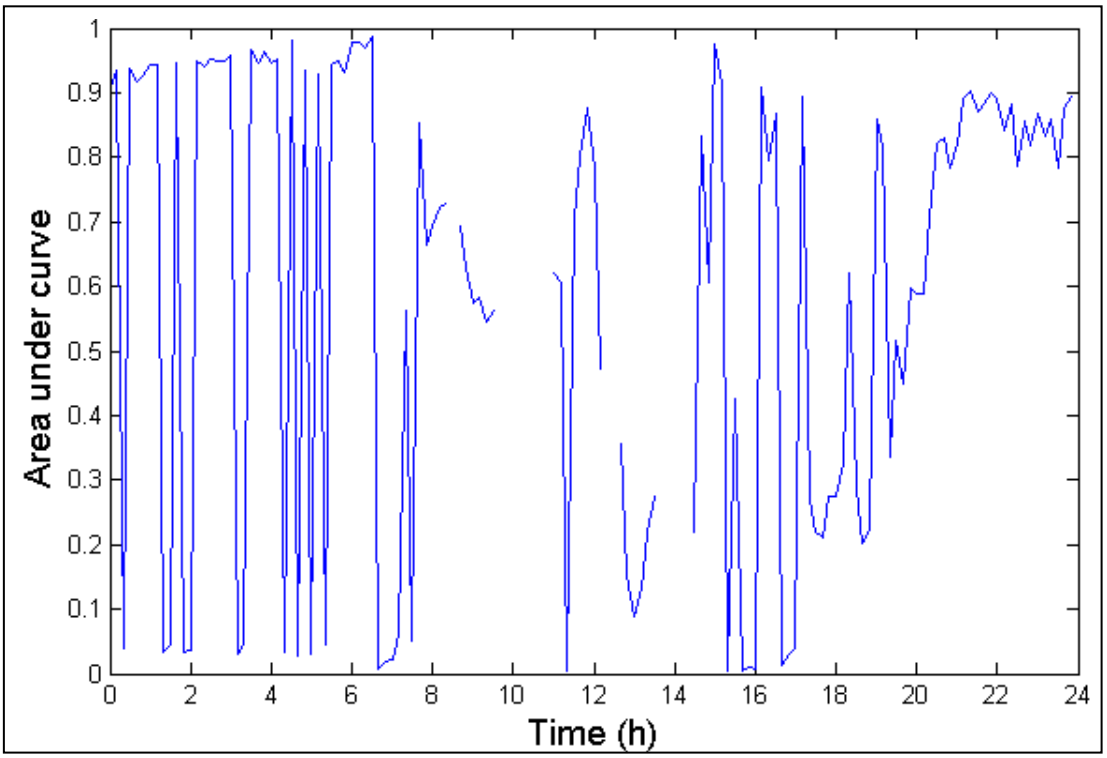

Figure 3. Diurnal ROC curve analysis for PC 1.

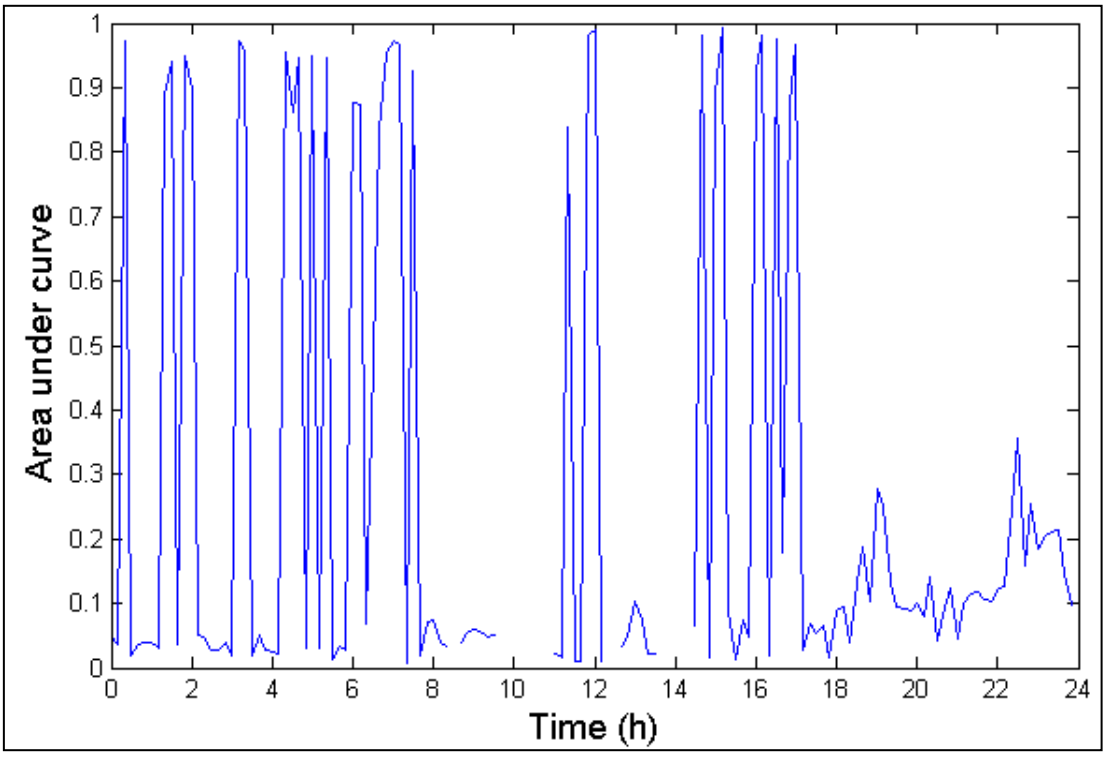

Figure 4. Diurnal ROC curve analysis for PC 2.

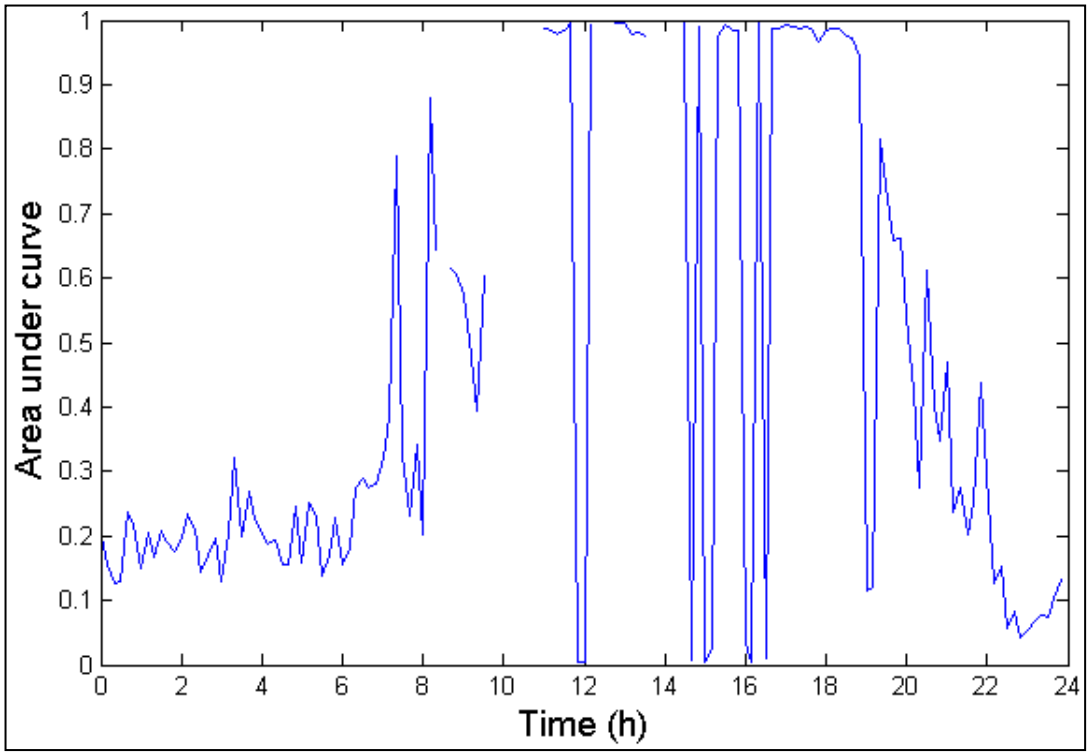

Figure 5. Diurnal ROC curve analysis for PC 3.

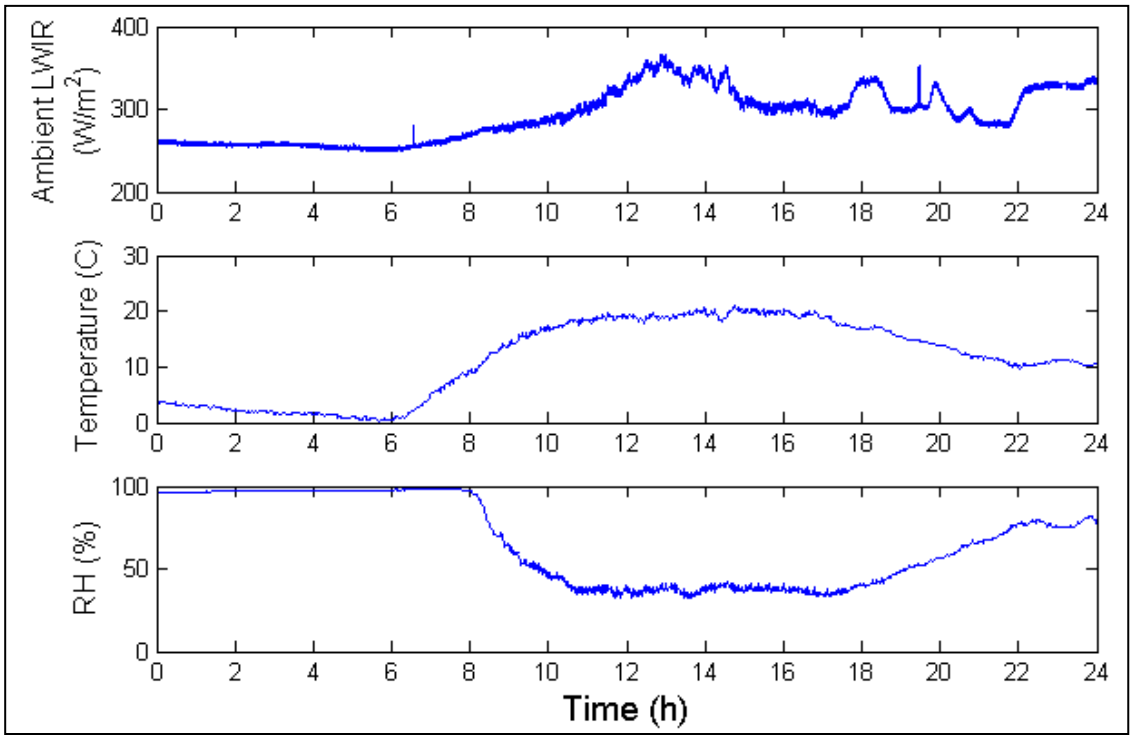

Figure 6. Environmental parameters measured during the test.

There appear to be at least two factors that limit PCA's usefulness for efficient image fusion. First, the shifting of the periods of high area under the curve between the PCs may be due to the inherent noise levels of the microbolometer-based camera. This claim is supported by the fact that stable area under the ROC curves occurs during the daytime hours, which corresponds to times of maximum signal levels and lasts for approximately 3 h, while the stable periods at night, or during low signal levels, only last for 1 h. Second, the accuracy of the ROC curve metric for assessing the contrast within the PC images calculated from S_0, S_1, and S_2 images suffers from the diversity of the S_0, S_1, and S_2 signatures of the objects within the scene. This diversity, combined with the variability in the weighting factors and correlations used in the calculation of the PCs, often results in significant overlap of target and background histograms. As explained previously, ROC curve analysis alone is not a good metric to use in such a scenario due to its inability to account for pixel clustering corresponding to objects within the scene. In this case, a more traditional contrast metric, e.g., the normalized difference between mean target and background values, may be more applicable.

4.2 Fused S_0 and Enhanced DOLP

The diurnal plots of area under the ROC curve for DOLP and enhanced DOLP are presented in figure 7. Comparison of the area under the ROC curve for the DOLP imagery with the ambient IR loading presented in figure 6 shows that the contrast between manmade targets and their backgrounds in DOLP imagery decreases as ambient levels of IR radiation increase due to clouds. This finding is similar to the relationship between LWIR S_1 polarimetric signatures and ambient IR loading shown in Felton et al., 2010 (*9*). In addition, it is shown in figure 7 that the enhanced DOLP contrast is much less susceptible to the effects of the ambient IR loading. This is mainly because in this scene, the S_2 data is much less susceptible to the effects of optical background; therefore, the enhanced DOLP conveys more S_2 information than the conventional DOLP.

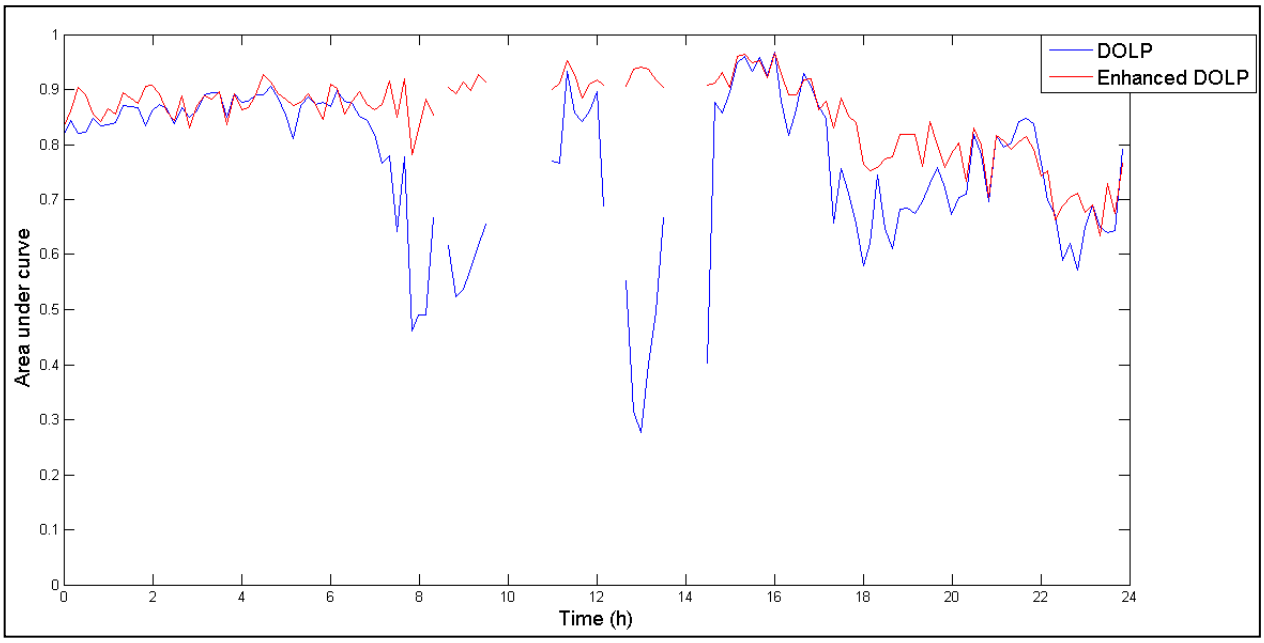

Figure 7. Diurnal DOLP and enhanced DOLP ROC curve analysis.

Figures 8 and 9 allow for a comparison of example DOLP and enhanced DOLP imagery used to obtain the results of the ROC curve analysis presented in figure 7. Figure 8 shows the DOLP and enhanced DOLP images taken at 0000 while figure 9 shows the imagery taken at 1300. As shown in figure 8, the contrast for the manmade targets defined in figure 2 is very similar in the DOLP and enhanced DOLP images taken at 0000. This is consistent with the results of the ROC curve analysis at 0:00 in figure 7. On the other hand, figure 7 indicates a decrease in the DOLP contrast at 1300 that we have shown earlier to be due to the optical background whose source is the clouds. Meanwhile, the high area under the ROC curve for enhanced DOLP is maintained during this same period. Figure 9 shows that this difference in contrast is due mostly to the disappearance of the road in the DOLP image, although some differences in the contrast of the surrogate tanks is observed, as well.

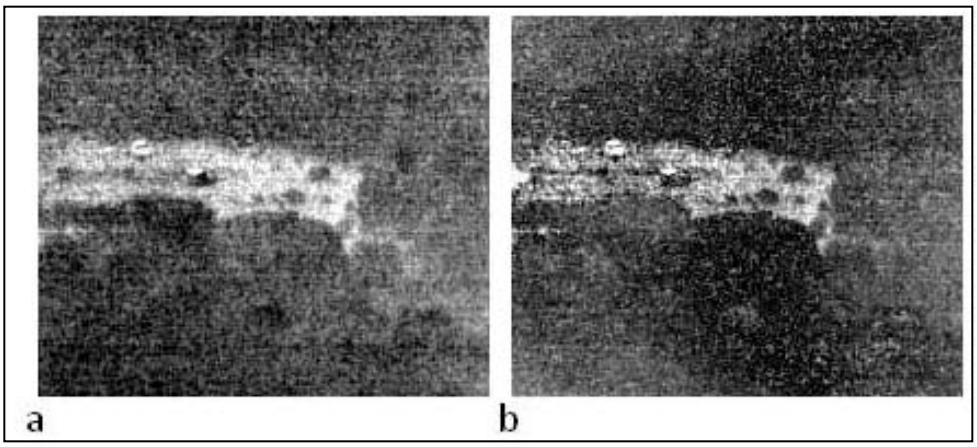

Figure 8. DOLP (a) and enhanced DOLP (b) images taken at 0:00.

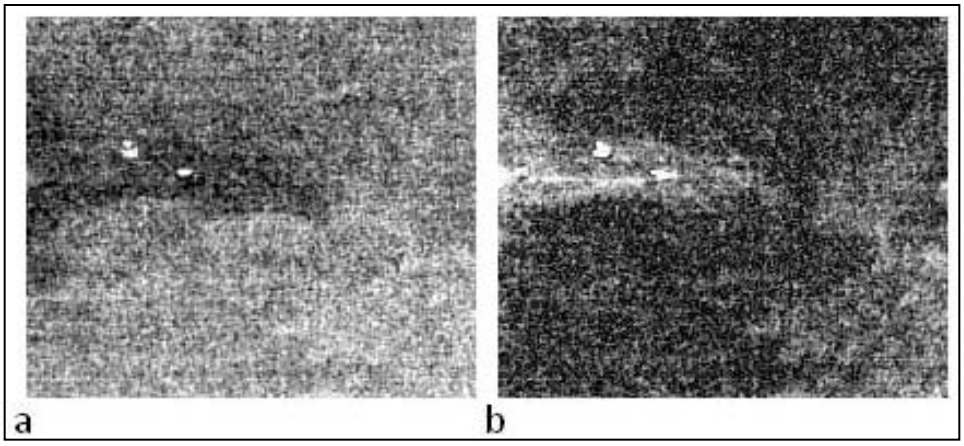

Figure 9. DOLP (a) and enhanced DOLP (b) images taken at 13:00.

The diurnal plots of area under the ROC curve for S_0 and fused S_0-enhanced DOLP are presented in figure 10. From 0000 to 0700, temperatures were less than 5 °C and slowly decreasing, while the skies were clear and the relative humidity was consistently 95–99%. During this time, the area under the fused S_0-enhanced DOLP ROC curves was, on average, 20% higher than the area under the S_0 ROC curves. Figure 11 provides a comparison of the S_0 and fused S_0-enhanced DOLP imagery. During the majority of the pre-dawn hours, there was very little contrast between the surrogate tanks, and the trees and bushes in the S_0 images. The fusion of the enhanced DOLP information to the S_0 image significantly improved upon this particular contrast. After the sun rose and the scene began to heat up, the difference between the fused S_0-enhanced DOLP and S_0 area under the ROC curve began to decrease. This was expected because sufficient thermal contrast between the targets and their backgrounds had been achieved.

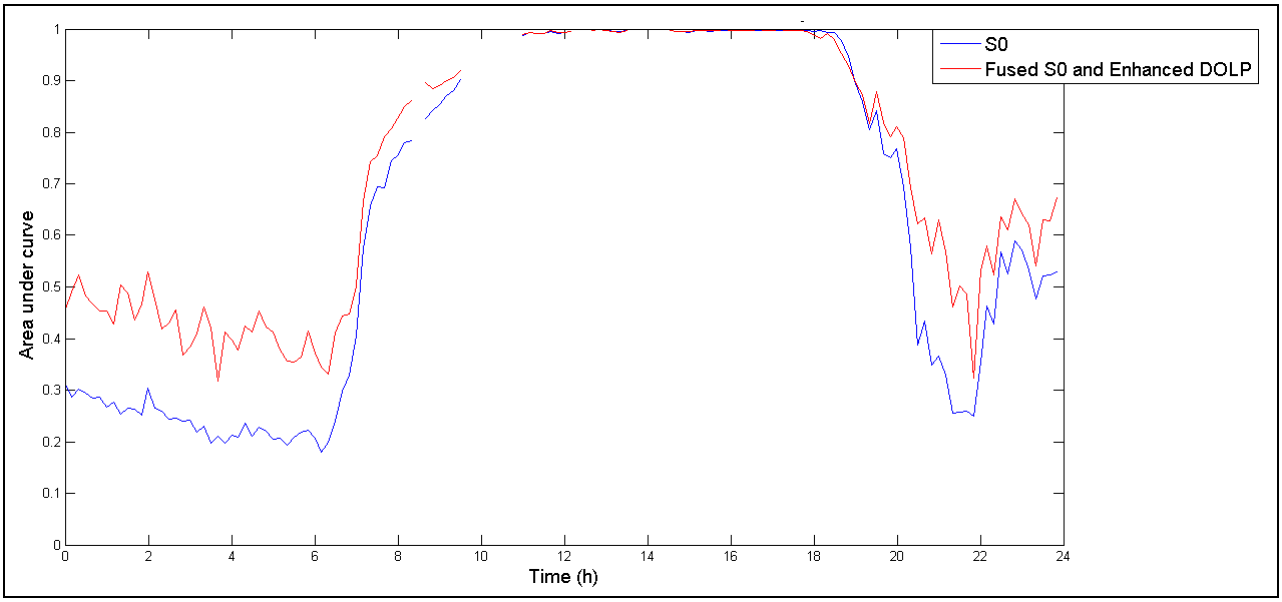

Figure 10. Diurnal S_0 and fused S_0-enhanced DOLP ROC curve analysis.

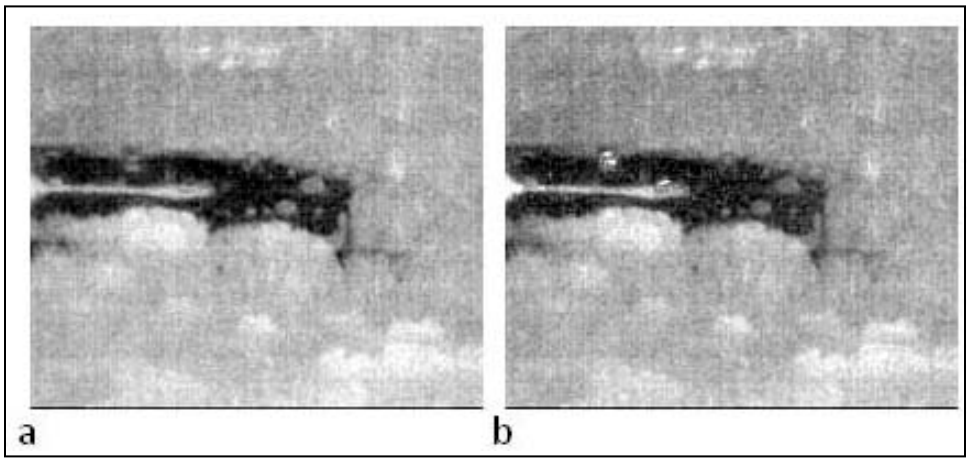

Figure 11. S_0 (a) and fused S_0-enhanced DOLP (b) images taken at 0:00.

The sun set at approximately 2000, and shortly thereafter, the cloud cover changed from partly cloudy to overcast, as indicated by the ambient IR loading in figure 6. During this time, thermal contrast between targets and background decreased once again, and both the DOLP and enhanced DOLP imagery became noisy due to the low polarimetric signal levels cause by the cloud-produced optical background. During this time, contrast between targets and backgrounds was maintained significantly better in enhanced DOLP imagery than in conventional DOLP imagery. Consequently, this information improved overall target contrast within the fused S_0-enhanced DOLP imagery, as illustrated in the diurnal ROC curve analysis plots between 2000 and 2350. Figure 12 further illustrates the improved contrast of enhanced DOLP and fused S_0-enhanced DOLP over conventional DOLP and S_0, respectively.

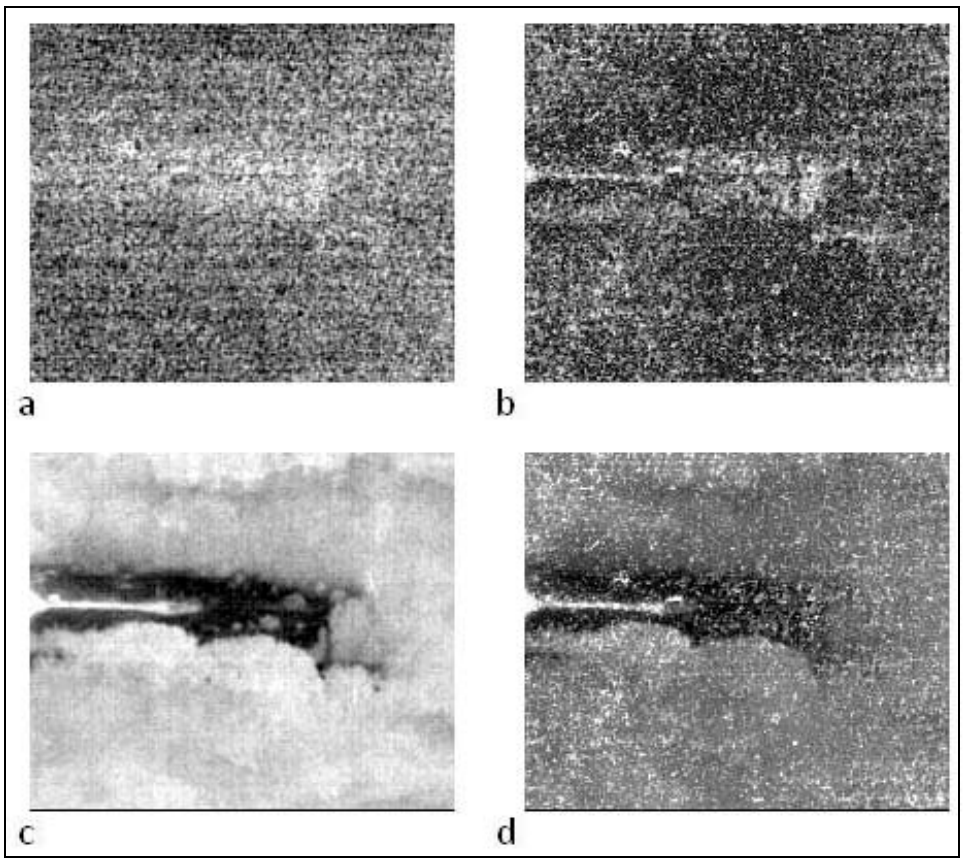

Figure 12. DOLP (a), enhanced DOLP (b), S_0 (c), and fused S_0-enhanced DOLP (d) images taken at 23:50.

5. Conclusion

Due to the multivariate output of today's polarimetric imagers, there is a need to consolidate information to improve the efficiency of missions employing such a sensor. In this study, we have examined the use of two image fusion techniques to consolidate this information. The PCs resulting from PCA proved to be inadequate for conveying consistent contrast information between targets and backgrounds. The end result is that the information provided by the sensor is not consolidated because analysis of all the PCs must still be performed.

On the other hand, fusing the novel enhanced DOLP, which proved to be much less susceptible to the effects of the optical background than conventional DOLP, with the S_0 image provided a robust data product that sufficiently combines the information provided by the sensor. Using ROC curve analysis, we have shown that this data product enhances conventional thermal imagery by providing contrast between manmade targets and their natural background during periods of low thermal contrast, as well as during periods of high optical background.

Lastly, much care must be exercised when using the area under the ROC curve as a contrast metric. This metric does not perform well when there is significant overlap of target and background histograms because it fails to account for the clustering of pixels that correspond to objects in the scene. Therefore, future studies that aim to quantify contrast should find a more comprehensive metric, or use ROC curve analysis in combination with an additional metric, that can account for the clustering of pixels.

6. References

1. Shumaker, D. L.; Wood, J. T.; Thacker, C. R. Infrared Imaging Systems Analysis, DCS Corporation, Alexandria, 2-45–2-49, 1993.

2. Tyo, J. S.; Goldstein, D. L.; Chenault, D. B.; Shaw, J. A. Review of Passive Imaging Polarimetry for Remote Sensing Applications. *App. Optics* **2006**, *45* (22), 5453–5469.

3. Tyo, J. S.; Pugh, E. N.; Engheta, N. Colorimetric Representations for Use with Polarization-difference Imaging of Objects in Scattering Media. *J. Opt. Soc. Am. A* **1988**, *15* (2), 367–374.

4. Pohl, C.; Van Genderen, J. L. Multisensor Image Fusion in Remote Sensing: Concepts, Methods and Applications. *Int. J. Remote Sensing* **1998**, *19* (5), 823–854.

5. Pezzaniti, J. L.; Hyatt, B.; Reinhardt, J. *Systems Users Manual: LWIR Rotating Retarder Imaging Polarimeter*, 2008.

6. Dillon, W. R.; Goldstein, M. *Multivariate Analysis: Methods and Applications*; John Wiley & Sons, New York, Chichester, Brisbane, Toronto, and Singapore, 23–50, 1984.

7. Singh, A.; Harrison, A. Standardized Principal Components. *Int. J. Remote Sensing* **1985**, *6* (6), 883–896.

8. Hanley, J. A.; McNeil, B. J. The Meaning and Use of the Srea Under a Receiver Operating Characteristic (ROC) Curve. *Radiology* **1982**, *143* (1), 29–36.

9. Felton, M.; Gurton, K. P.; Pezzaniti, J. L.; Chenault, D. B.; Roth, L. E. Comparison of the crossover periods for mid- and long-wave IR (MidIR and LWIR) polarimetric and conventional thermal imagery. submitted to *SPIE*, Orlando, FL, April 5–9, 2010.

List of Symbols, Abbreviations, and Acronyms

ARDEC	Armament Research and Development Engineering Center
DOLP	degree-of-linear polarization
IR	infrared
LWIR	long-wave IR
PAL	Precision Armament Laboratory
PIR	precision infrared radiometer
PCs	Principal components
PCA	principal component analysis
ROC	receiver operating characteristic

No. of Copies	Organization
1 ELECT	ADMNSTR DEFNS TECHL INFO CTR ATTN DTIC OCP 8725 JOHN J KINGMAN RD STE 0944 FT BELVOIR VA 22060-6218
1 CD	OFC OF THE SECY OF DEFNS ATTN ODDRE (R&AT) THE PENTAGON WASHINGTON DC 20301-3080
1	US ARMY RSRCH DEV AND \ ENGRG CMND ARMAMENT RSRCH DEV & ENGRG CTR ARMAMENT ENGRG & TECHNLGY CTR ATTN AMSRD AAR AEF T J MATTS BLDG 305 ABERDEEN PROVING GROUND MD 21005-5001
1	PM TIMS, PROFILER (MMS-P) AN/TMQ-52 ATTN B GRIFFIES BUILDING 563 FT MONMOUTH NJ 07703
1	US ARMY ABERDEEN TEST CENTER ATTN TEDT AT WFT F CARLEN 400 COLLERAN ROAD ABERDEEN PROVING GROUND MD 21005-5009
1	US ARMY CECOM RDEC NVESD ATTN AMSRD CER NV ST SIP J HOWE 10221 BURBECK RD STE 430 FT BELVOIR VA 22060-5806
1	US ARMY INFO SYS ENGRG CMND ATTN AMSEL IE TD A RIVERA FT HUACHUCA AZ 85613-5300

No. of Copies	Organization
1	COMMANDER US ARMY RDECOM ATTN AMSRD AMR W C MCCORKLE 5400 FOWLER RD REDSTONE ARSENAL AL 35898-5000
3	US ARMY RDECOM ARDEC ATTN AMSRD AAR MEF S L E ROTH ATTN M WOOLLEY ATTN AMSRD AAR AEP S J ROMANO BLDG 407 PICATINNY ARSENAL NJ 07806-5000
1	US ARMY TARDEC ATTN AMSRD TAR MS 263 G GRANT 6501 EAST 11 MILE RD WARREN MI 48397-5000
1	AFRL/RYJT ATTN R T MACK 2241 AVIONICS CIRCLE BLDG 620 WRIGHT-PATTERSON AFB OH 45433-7320
3	AFRL/VS ATTN T R CAUDILL ATTN M J DUGGIN ATTN M FETROW 3550 ABERDEEN SE KIRTLAND AFB NM 87117
1	US GOVERNMENT PRINT OFF DEPOSITORY RECEIVING SECTION ATTN MAIL STOP IDAD J TATE 732 NORTH CAPITOL ST NW WASHINGTON DC 20402
1	JOHNS HOPKINS UNIVERSITY APPLIED PHYSICS LAB ATTN MP3-W110 A GOLDBERG 11100 JOHNS HOPKINS RD LAUREL MD 20723-6099

No. of Copies	Organization
2	COLLEGE OF OPTICAL SCIENCES UNIVERSITY OF ARIZONA ATTN B M RATLIFF ATTN S TYO TUCSON AZ 85721
1	GEORGIA TECH RSRCH INSTITUTE ATTN J S ACCETTA 2015 YALE BLVD SE ALBUQUERQUE NM 87106
1	MONTANA STATE UNIVERSITY ATTN J SHAW 108 CULBERTSON HALL P.O. BOX 172000 BOZEMAN MT 59717-2000
2	POLARIS SENSOR TECHNOLOGIES INC ATTN D B CHENAULT ATTN J L PEZZANITI 200 WESTSIDE SQUARE STE 320 HUNTSVILLE AL 35801
1	US ARMY RSRCH LAB ATTN RDRL CIM G T LANDFRIED BLDG 4600 ABERDEEN PROVING GROUND MD 21005-5066
1	DIRECTOR US ARMY RSRCH LAB ATTN RDRL ROE V W D BACH PO BOX 12211 RESEARCH TRIANGLE PARK NC 27709
15	US ARMY RSRCH LAB ATTN IMNE ALC HRR MAIL & RECORDS MGMT ATTN RDRL CIE S K GURTON (5 COPIES) ATTN RDRL CIE S M FELTON (5 COPIES) ATTN RDRL CIM L TECHL LIB ATTN RDRL CIM P TECHL PUB ATTN RDRL SEE E K KLETT, JR. ATTN RDRL SER E R DEL ROSARIO ADELPHI MD 20783-1197
TOTAL:	41 (39 HCS, 1 PDF, 1 CD)